My current research focused on diffuse ionized gas started last summer, advised by Professor Lei Hao in Shanghai Astronomical Observatory, Chinese Academy of Science. Gas cycling plays an instrumental role in the galaxy ecosystem and reveals details in the process of galaxy evolution. Our project revolves around special emission-line properties in certain galaxies searched in SDSS-IV Mapping Nearby Galaxies at APO (MaNGA) survey, a multi-object IFU survey expected to target 10,000 galaxies by 2020.

The project origins from several galaxies in Lyman Break Analogs where galaxies are selected based on their far-UV properties and they show properties similar to those of high-redshift Lyman Break Galaxies. Overzier et al. 2009 found rare galaxies with unusual behavior on the plot of [NII]/[SII] versus [OIII]/[Hβ], which show extreme [NII]/[SII] similar to local IR-warm starbursts.

Additionally, Hao et al. (2014) studied anomalous dust properties in three galaxies found when cross-matching the SDSS and Spitzer/IRS low-resolution spectra, two of which overlap with these rare samples in LBAs. I work mainly on exploring the mechanism of the prominent [NII]/[SII] ratio.

Large Sample Study

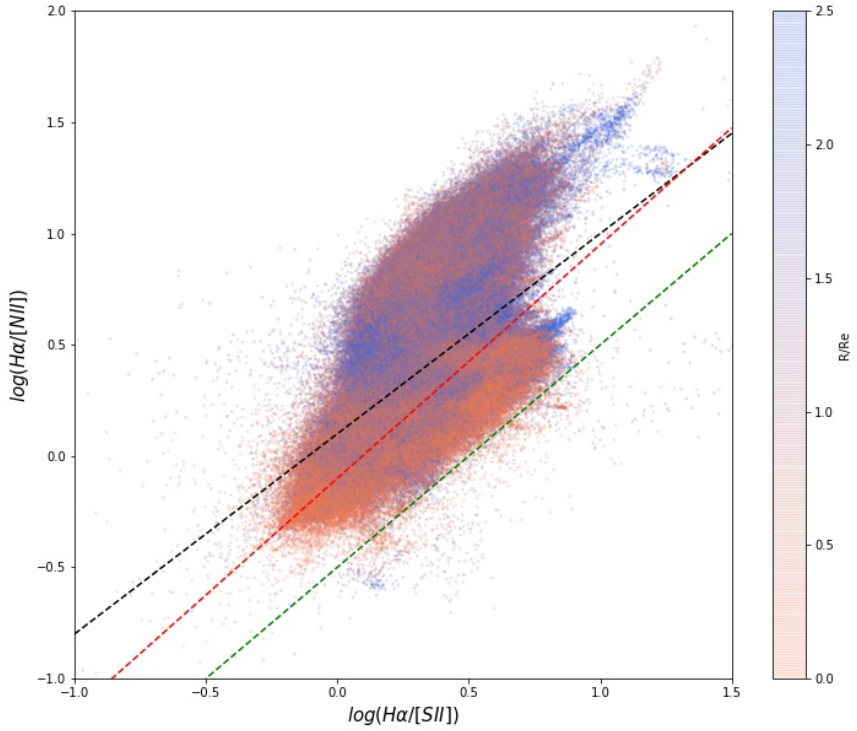

Figure 1. Map of H /[NII] and H /[SII] for MaNGA MPL-8 with emission lines in 5σ cut-off. The color denotes the relative distance from the spaxel to its host galaxy's center(R/Re). Black dash line: log([Hα]/[NII]) = 0.9 × log ([Hα]/[SII] + 0.1). Red dash line: log([Hα]/[NII]) = 1.05 × log ([Hα]/[SII]) - 0.1. Green dash line: log([Hα]/[NII]) = log ([Hα]/[SII]) - 0.5.

Obtaining the SDSS-MaNGA MPL-8 data of 6500 galaxies, I track their line properties by mapping [Hα]/[NII] - [Hα]/[SII] with emission lines in 5σ cut-off (Fig 1), which may indicate

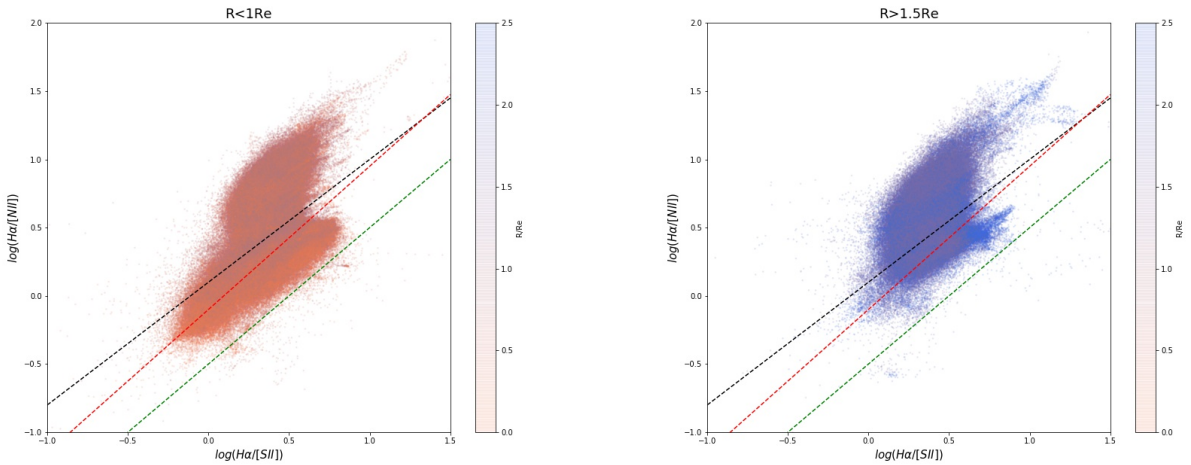

Figure 2. *Left:* R<1Re, *Right:* R>1.5Re

different mechanisms for diffuse ionized gas (Lam et al., in prep.). The ionization potential of [NII] and [SII] are close to each other (e.g. 14.53 eV of [NII] and 10.36 eV of [SII]), indicating similar excitation states. Lam et al. found different distribution for the [NII] and [SII] in NGC4013 by using data from VIRUS-P Exploration of Nearby Galaxies Survey (VENGA) and concluded that they are account for different excitation mechanisms. The black dash line in Fig 1 is identical to their by-eye separation line of excitation mechanism for NGC4013. The green dash line in Fig 1 is equivalent to the vertical line in Fig **??**. The black dash line is a by-eye estimate of our data.

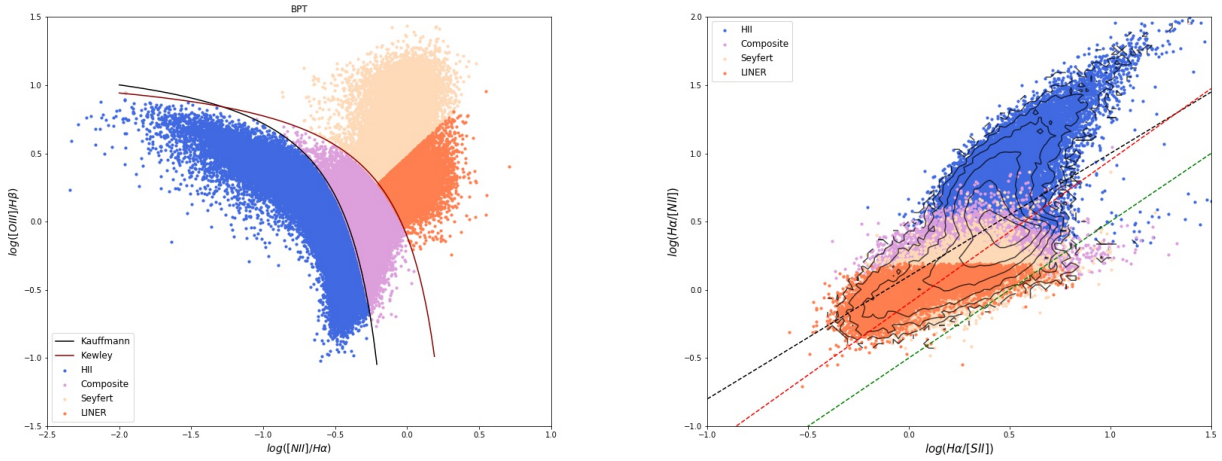

Figure 3. *Left:* BPT diagnostics of SDSS DR7 data. *Right:* Map of Hα/[NII] and Hα/[SII] for SDSS DR7. Blue: star-forming galaxies. Pink: Composite galaxies. Yellow: Seyfert. Orange: LINERs.

Lam et al. also explored whether different distributions of [NII] and [SII] are common in galaxies using SDSS DR7 data. We repeat their map of SDSS DR7 data in Fig 3. The left panel shows the BPT diagnostics for each data point indicating the galaxy center. The right panel shows the [Hα]/[NII] - [Hα]/[SII] map with colors identical to their BPT classification.

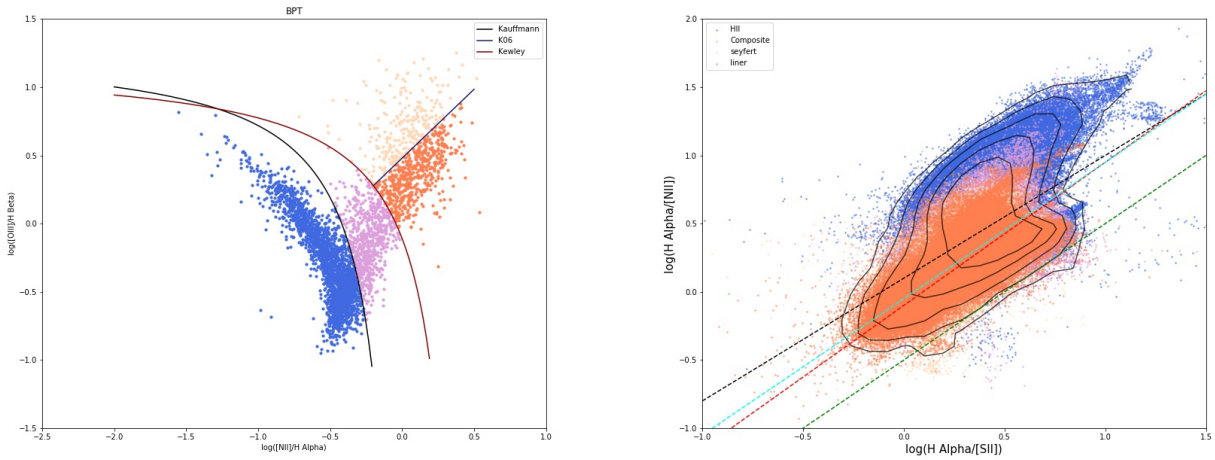

Figure 4. *Left:* BPT diagnostics of MaNGA MPL-8 data. Each point denotes a spaxel of a galaxy. The classification is based on the center spaxel. *Right:* Map of Hα/[NII] and Hα/[SII] for MaNGA MPL-8. Blue: star-forming galaxies. Pink: Composite galaxies. Yellow: Seyfert. Orange: LINERs.

For MaNGA MPL-8 data, we classify spaxels according to their host galaxies' classifications, i.e. the BPT diagnostics of the central spaxel, and mapped [Hα]/[NII] - [Hα]/[SII](Fig 4). We adopt (log ([Hα]/[NII]) = log ([Hα]/[SII]) - 0.05) (light blue line in Fig 4) as a new reference between black dash line and red dash line.

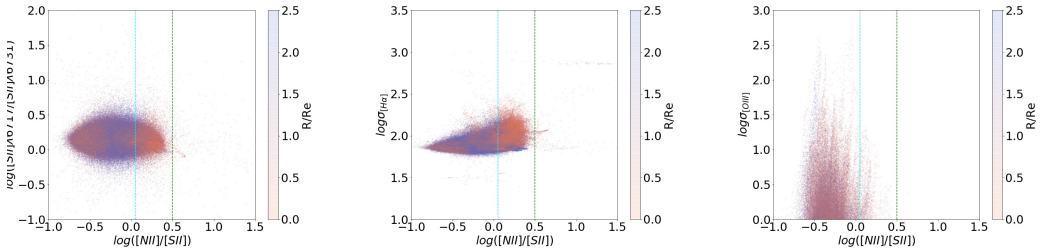

(a) SII ratio (b) $\sigma_{H\alpha}$ (c) $\sigma_{[OIII]}$

Figure 5. Spaxels in galaxies classified as star-forming or composite. (a) [SII] 6718/[SII] 6732–[NII]/[SII]. (b) σ[H] –[NII]/[SII]. (c) σ[OIII] –[NII]/[SII]. Green dash line: log([NII]/[SII])=0.5. Light blue dash line: log([NII]/[SII])=0.05.

In an effort to figure out the impact of electron density to the extreme [NII]/[SII], we exclude spaxels from galaxies classified as Seyfert or LINER and mapped the [SII]λ6718/[SII]λ6732, $\sigma_{[H\alpha]}$ and $\sigma_{[OIII]}$ over [NII]/[SII] for residual star-forming and composite galaxies (Fig 5).

We also plot BPT diagnostics based on the emission line properties for each spaxel and mapped the same properties(Fig 6). Both show no significant reliance on density for prominent [NII]/[SII].

Extreme Starbursts Candidates

We then try to find extreme [NII]/[SII] representative galaxies. We divide the [Hα]/[NII] - [Hα]/[SII] map of MaNGA into three branches. First branch: above log ([Hα]/[NII]) = log ([Hα]/[SII]) - 0.05 (light blue dash line). Second branch: between (log ([Hα]/[NII]) = log ([Hα]/[SII])

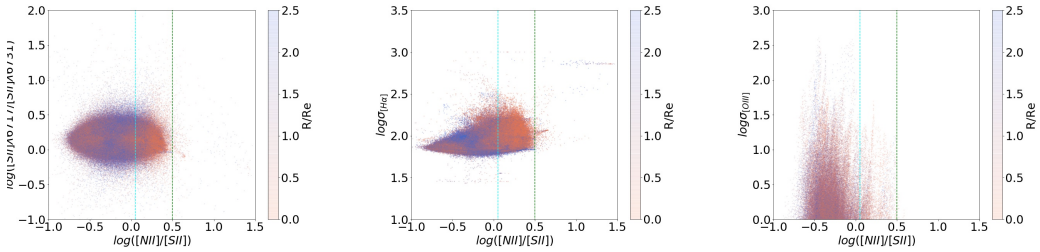

(a) SII ratio (b) $\sigma_{H\alpha}$ (c) $\sigma_{[OIII]}$

Figure 6. Spaxels with emission properties classified as star-forming or composite.

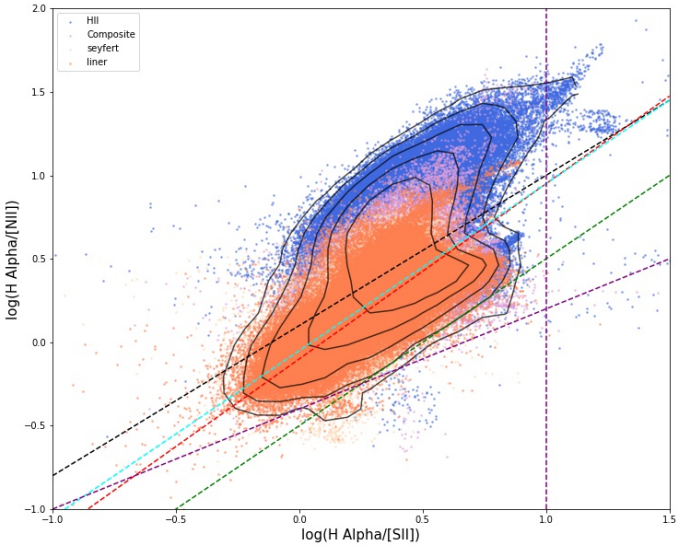

Figure 7. Purple dash lines confine the populated region in third branch together with the green dash line.

- 0.05) and (log ([Hα]/[NII]) = log ([Hα]/[SII]) - 0.5) (green dash line). Third branch: below: (log ([Hα]/[NII]) = log ([Hα]/[SII]) - 0.5). In Fig 7, we define a populated area in high-[NII]/[SII] zone(Third Branch) and select galaxies with more than 10 spaxels in the zone. Among these 14 galaxies, we extract their spectra from central spaxel and select three galaxies with star-forming characteristics: PLATE-IFU=8078-6104, PLATE-IFU=8989-1902 and PLATE-IFU=7960-12705.

We show their SDSS image, Branch map(spaxels shown in different branches), BPT map and [Hα]/[NII] - [Hα]/[SII] map in the top panel in Fig 8, Fig 10 and Fig 12 with [Hα] flux map, velocity dispersion maps of [Hα] and [OIII], [SII]λ6718/[SII]λ6732 map and [Hα] velocity map in the bottom panel. Their central spaxel spectra are shown in Fig 9, Fig 11 and Fig 13.

In particular, we are surprised to find that in the map of PLATE-IFU=7960-12705, the extreme [NII]/[SII] region (spaxels of the Third Branch) is off the center. In Fig 14, we spot a spaxel in the region and show its spectrum in Fig 15.

Currently, I work on extracting the Na I D spectroscopy from those with target characteristics to see the impact of outflows and also giving an overview of outflows in the MaNGA samples, e.g., how widespread they are and the scope of their impacts.

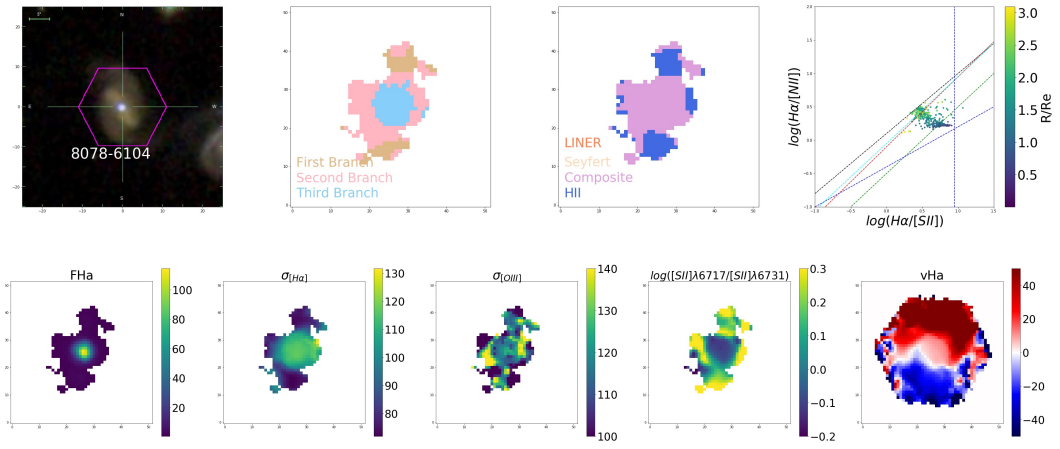

Figure 8. PLATE-IFU=8078-6104, z= 0.0442102. *Top:* (1) SDSS image. (2) Branch map. (3) BPT map. (4) [Hα]/[NII] - [Hα]/[SII] map. *Bottom:* (1) Hα flux. (2) $\sigma_{[H\alpha]}$map. (3)$\sigma_{[OIII]}$map. (4) log([SII]λ6718/[SII]λ6732) map. (5) v[Hα] map.

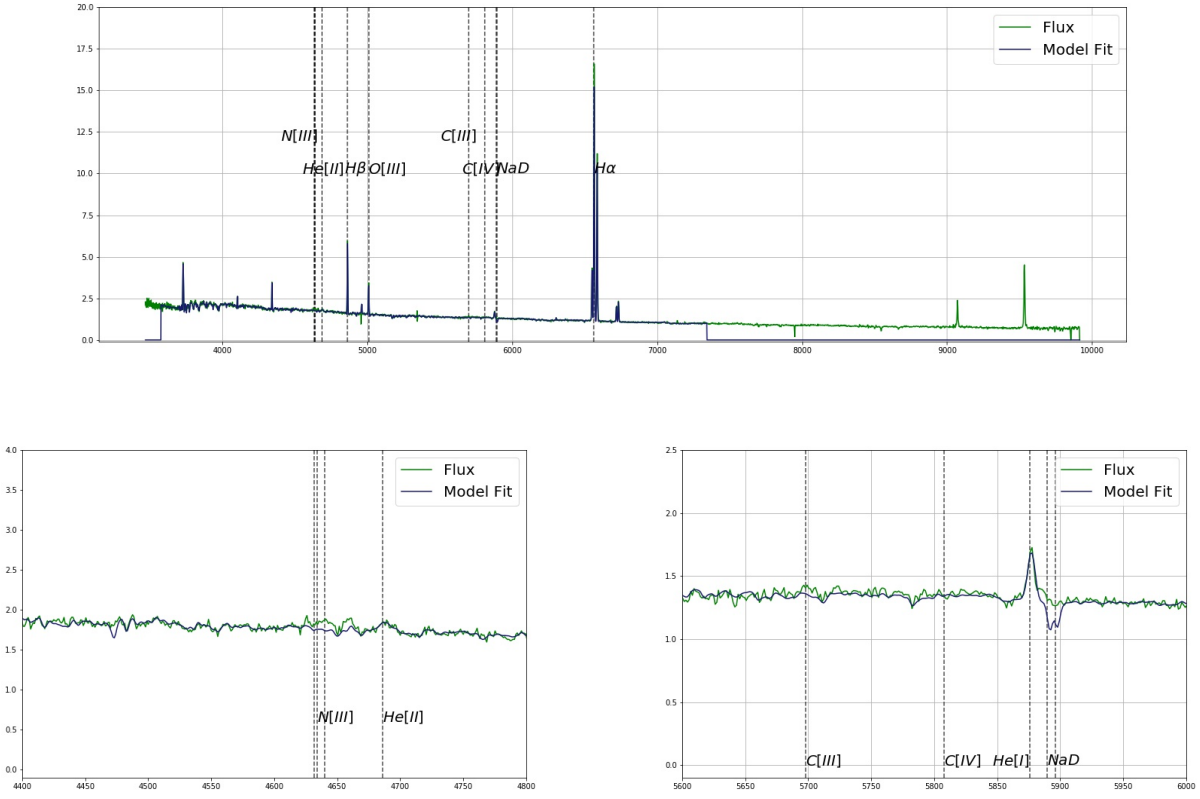

Figure 9. Central spaxel spectrum of PLATE-IFU=8078-6104.

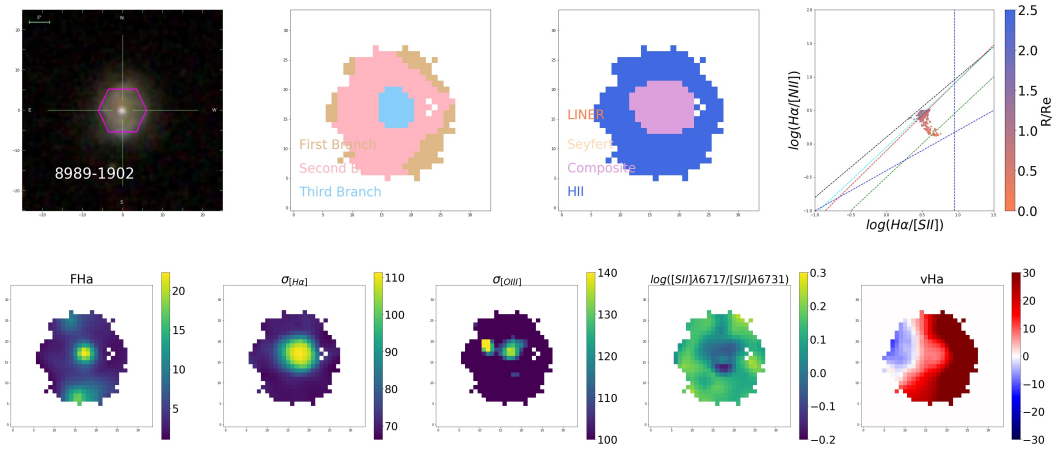

Figure 10. PLATE-IFU=8989-1902, z= 0.0530696.

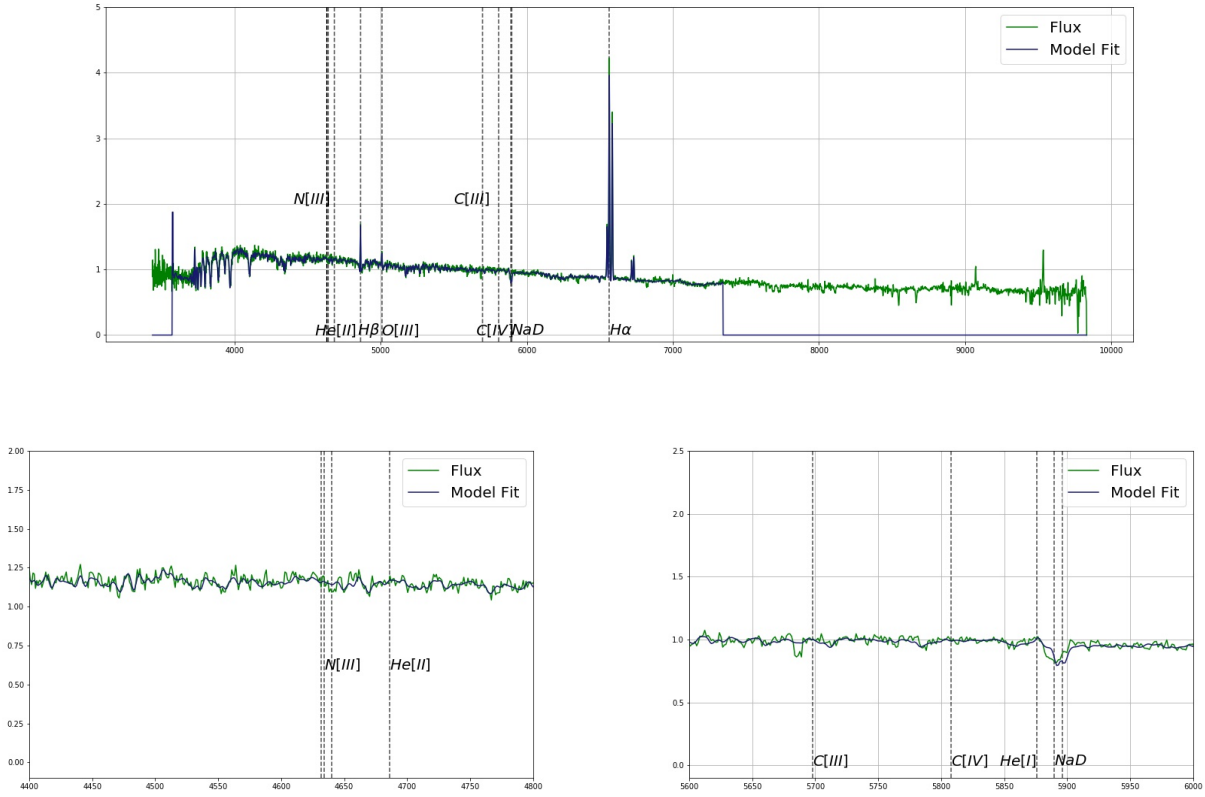

Figure 11. Central spaxel spectrum of PLATE-IFU=8989-1902

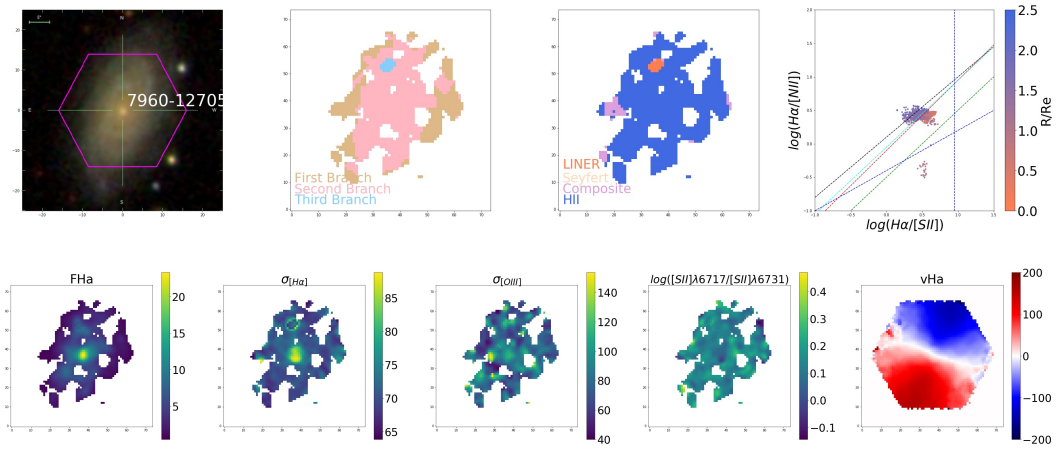

Figure 12. PLATE-IFU=7960-12705, z= 0.0295939.

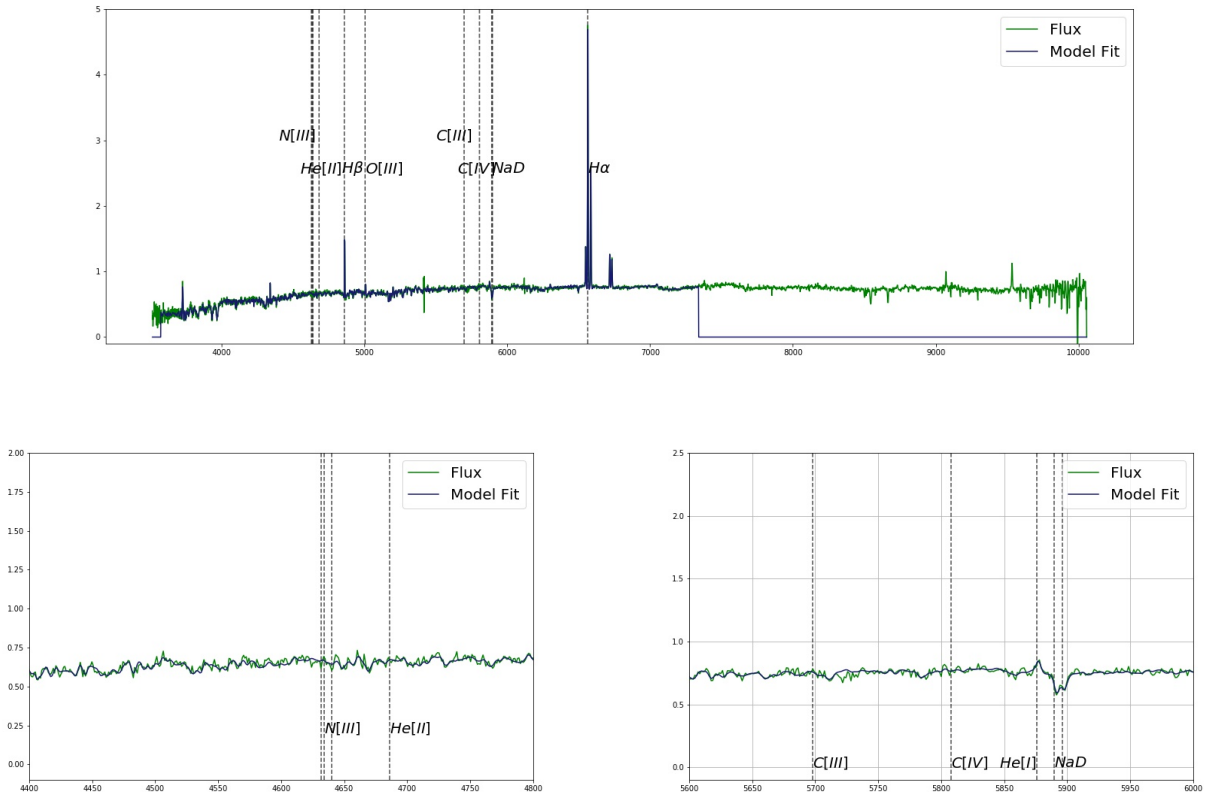

Figure 13. Central spaxel spectrum of PLATE-IFU=7960-12705.

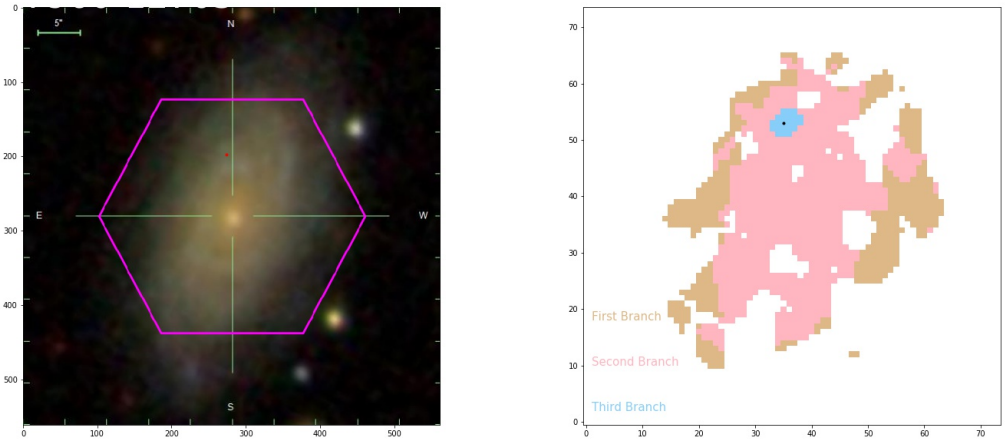

Figure 14. The spotted spaxel noted as red dot(Left) and black dot(right).

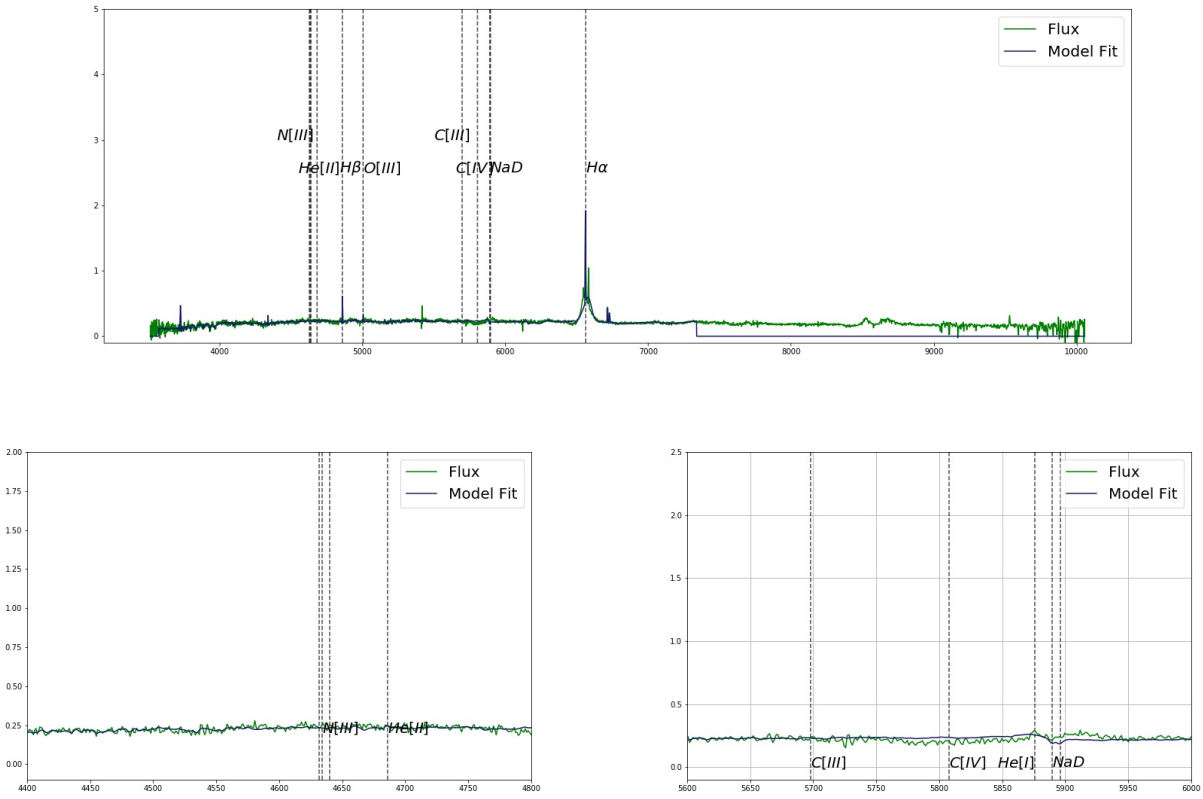

Figure 15. Spotted spaxel spectrum.

References

Overzier RA, Heckman TM, Tremonti C, Armus L, Basu-Zych A, et al. 2009. Astrophys. J. 706(1):203–22

Xie Y, Hao L, Li A. 2014. Astrophys. J. Lett. 794(2):